

Risks associated with laser radiation reflections in a healthcare environment: a surface reflectance study in the range 250 nm-25 μ m

Giacomo Insero,¹ Luca Mercatelli,² Maria Cristina Cimmino,³ Roberto Gaetano Donato,¹ Giovanni Romano,^{1,4} Franco Fusi,^{1,4} Andrea Guasti³

¹Department of Experimental and Clinical Biomedical Sciences “Mario Serio”, University of Florence, Florence; ²National Institute of Optics, CNR, Florence; ³UOC Fisica Sanitaria USL Toscana Sud Est, Siena; ⁴Probiomedica srl, Florence, Italy

Abstract

Biomedical applications relying on optical radiation, particularly with the advent of lasers, have experienced exponential growth in the last 20 years. Powerful optical sources are now

Correspondence: Giovanni Romano, Department of Experimental and Clinical Biomedical Sciences “Mario Serio”, University of Florence, Viale G. Pieraccini 6, 50139 Florence, Italy.
E-mail: giovanni.romano@unifi.it

Key words: laser safety, specular reflectance, ocular hazard.

Contributions: GI, data collection, data analysis, manuscript interpretation, and draft; LM, data collection, data analysis, critical revision of the article; MCC, data collection, data analysis; RGD, data collection; GR, manuscript interpretation, critical revision of the article; FF, conceptualization, data analysis; AG, critical revision of the article, final approval.

Conflict of interest: the authors declare no potential conflict of interest, and all authors confirm accuracy.

Ethics approval: not applicable.

Informed consent: not applicable.

Patient consent for publication: not applicable.

Conference presentation: some data in the work were presented at the conference AIFM National Congress on 8-11 June 2023, Florence Italy. Abstracts/Physica Medica 115S1 (2023) S1–S169.

Availability of data and materials: all data generated or analyzed during this study are included in this published article.

Acknowledgments: the research activity reported in this manuscript has been performed in the framework of the regional project “Suppression of Airborne Viral Epidemic Spread by Ultraviolet light Barriers (SAVES-US)” and the project “Endoscopio luminoso per il trattamento dell’*Helicobacter pylori* (EndoLight)”, POR FESR 2014-2020. These research projects are funded by the Tuscany Region.

Received: 11 July 2024.

Accepted: 11 July 2024.

Early access: 25 July 2024.

This work is licensed under a Creative Commons Attribution 4.0 License (by-nc 4.0).

©Copyright: the Author(s), 2024
Licensee PAGEPress, Italy
Healthcare in Low-resource Settings 2024; 12:12802
doi:10.4081/hls.2024.12802

Publisher's note: all claims expressed in this article are solely those of the authors and do not necessarily represent those of their affiliated organizations, or those of the publisher, the editors and the reviewers. Any product that may be evaluated in this article or claim that may be made by its manufacturer is not guaranteed or endorsed by the publisher.

found not only in universities, hospitals, and industries but also in beauty centers, used for tasks such as tattoo removal, and even in our homes. Despite their widespread use, managing the risks associated with lasers, particularly in non-research contexts, has not kept pace with their proliferation. While the risks associated with direct exposure to radiation to the eye and skin are relatively well understood, the hazards posed by reflected and diffuse radiation remain less characterized and monitored. Therefore, there is a critical need to assess potential eye and skin hazards in spaces where lasers and non-coherent light sources are used. This necessitates a detailed analysis of reflective surfaces, with particular emphasis on evaluating their reflectance characteristics at relevant wavelength ranges. This study investigates the reflectance and transmittance (where relevant) properties of commonly used materials in biomedical settings, including fabrics, plastics, and metals, across a broad spectrum from 250 nm (UVA) to visible light and into the infrared (IR) region up to 25 μ m. Both specular (at 45° incidence) and diffuse reflectance spectra were measured using spectrophotometric techniques and used to provide a straightforward parameter to classify the specular/diffusive behavior of the different surfaces. Besides, small-angle reflectance measurements in the IR range were performed by Fourier transform infrared spectrometry. The knowledge of the material optical properties used in environments where optical radiation is employed allows for accurate assessment of associated risks. This facilitates the determination of appropriate preventive measures and the establishment of safer protocols, for both operators and, where applicable, patients and the general public. For this scope, the creation of a database of material reflective properties has been initiated.

Introduction

The current legislation in various countries mandates the assessment of risks posed by physical agents such as optical radiation from artificial sources.¹⁻⁴ Accordingly, it is necessary to implement technical and procedural measures to mitigate these risks comprehensively. This necessitates a full examination of all potential ocular and dermal hazards in facilities where lasers and non-coherent sources are used.^{5,6} Special attention must be focused on all the reflective surfaces that could be exposed to the light source by the operator, whether intentionally or not. It is crucial to account for the surface reflectance at the specific emission wavelength of the source

Existing experimental studies on materials in clinical environments are limited, and a comprehensive database of surface reflective properties for risk management is currently lacking,⁷ also considering innovative light sources.⁸ Further research in this field is then evidently necessary. This study aims to identify effective optical parameters for characterizing surfaces in risk assessment

and to establish straightforward methodologies for measuring these parameters in an easy but effective and accurate way. To achieve this goal, we analyzed many different materials that are commonly present in working environments where both lasers and non-coherent sources are utilized, including furnishings, clothing, and surface coverings, including analysis of different finishings of the same surface material (*e.g.*, polished versus satin-finished metals).

When light encounters an interface between two surfaces with a refractive index n discontinuity (being n defined as the ratio between the speed of light in vacuum and the speed of light in the medium), reflection, refraction, and scattering processes can occur. In this work, we mainly focus on light reflection at the interface between air and material, while a more detailed analysis of light-matter interaction can be found in.⁶ Depending on the surface characteristics, light can be reflected in either a specular or diffuse manner, as illustrated in Figure 1. While in the first case, reflection occurs at an angle θ_p equal to the angle of incidence θ_{pr} , in the diffusive case reflection occurs in all directions. Generally, all materials are capable of specular reflection if their surfaces are polished to reduce irregularities to a scale comparable to (or smaller than) the wavelength of the incident radiation. It is the surface roughness that is mainly responsible for backscattering. In practice, only metals can be efficiently polished to achieve almost a 100% specular reflection. In contrast, other common materials, even with the best-polished process, are mainly dominated by diffusive reflection, and only small fractions — generally 5-10% — of the incident radiation is specularly reflected, depending on the angle of incidence.

Contrary to common belief, the amount of reflected light from a medium is not solely due to the surface imperfections, but also involves backscattering from subsurface layers. This phenomenon underscores how scattered light provides insights into the surface layer structure of materials.

Materials and Methods

Fundamental to an accurate risk assessment of coherent and non-coherent light is the measurement and characterization of the optical properties of different materials. For this purpose, we need

to introduce the concepts of reflectance, transmittance, and absorbance.^{9,10} The total reflectance R_{Tot} of a material is a parameter that evaluates the fraction of the radiant flux incident on the material surface that is reflected. Similarly, if we consider the fraction that is transmitted, we can define the total transmittance T_{Tot} . All the leftover radiant flux that has not been either reflected or transmitted has been absorbed by the medium and defines the absorbance, which can be calculated in terms of R_{Tot} and T_{Tot} through the relation:

$$A(\lambda) = 1 - (R_{Tot}(\lambda) + T_{Tot}(\lambda)) \quad (1)$$

where we underlined the explicit dependence on the incident light wavelength λ . As previously discussed, the reflection of an incident beam involves specular reflection, where the reflectance and incident angles are equal, and diffuse reflection is scattered in all directions. The predominance of one or the other type depends on both the incident light wavelength and the surface properties, such as the material type and surface roughness degree. Since optical radiation risk assessment and safety measures can be different for specular and diffusive surfaces, the total reflectance can be decomposed as

$$R_{Tot}(\lambda) = R_S(\lambda) + R_D(\lambda) \quad (2)$$

where $R_S(\lambda)$ and $R_D(\lambda)$ represent the specular and diffusive reflectance, respectively. However, $R_S(\lambda)$ depends on the incidence angle of the light. To provide a measure of specular reflectance, we have decided to use a characteristic incidence angle of 45 degrees, identified by the symbol $R_S^{45^\circ}(\lambda)$. This angle is representative of many practical situations and is also easily measurable with simple and inexpensive setups, enabling even poorly equipped laboratories to extend or compare our measurements on other materials. The Eq. 2 now becomes:

$$R_{Tot}(\lambda) = R_S^{45^\circ}(\lambda) + R_D(\lambda) \quad (3)$$

Considering that the main purpose of this work is to make safe-

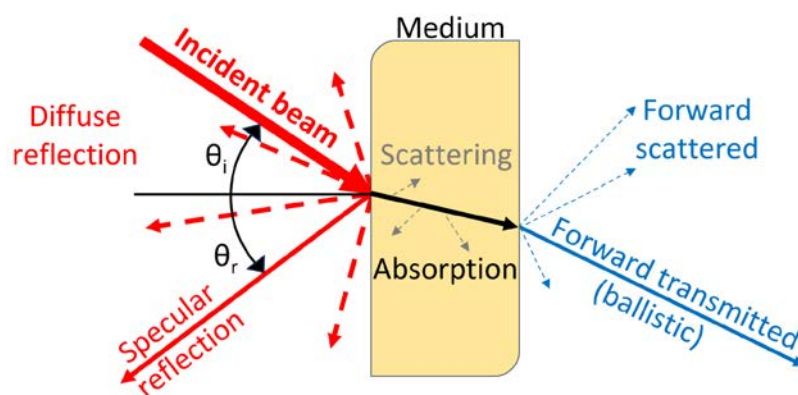


Figure 1. Scheme of the effects governing light transport in a medium.

ty officers aware of the risks of laser radiation reflecting off surfaces in healthcare environments, it is essential to identify a proper parameter that immediately indicates whether a surface mainly exhibits specular or diffusive characteristics. This can be identified by the Lambertian parameter $L_{LAMB}(\lambda)$ which can be obtained by measuring separately $R_S^{45^\circ}(\lambda)$ and $R_D(\lambda)$ and is defined as follows:

$$L_{Lamb}(\lambda) = 100 \cdot \left[\frac{R_S^{45^\circ}(\lambda)}{R_S^{45^\circ}(\lambda) + R_D(\lambda)} \right] \quad (4)$$

This parameter ranges from nearly 0 to 100; the more $L_{LAMB}(\lambda)$ approaches low values ($L_{LAMB}(\lambda)$ can be as low as zero, but in practical cases, it ranges between 1 to 100), the more diffusing the sample ($R_D \gg R_S^{45^\circ}$), while for a predominant specular behavior, $L_{LAMB}(\lambda)$ approaches 100 ($R_S^{45^\circ} = R_{TOT}$).

Since $L_{LAMB}(\lambda)$ is represented by a spectral curve, indicating its behavior as a function of wavelength, we will also provide a reference value for it, obtained as an average over the spectral range of 400-1100 nm and indicated as $L_{Lamb}^{400-1100\text{ nm}}$. Although this average value does not encompass all spectral information, it offers a practical alternative for an initial estimation of the specular or diffuse reflection behavior of a surface within the 400-1100 nm range. This range includes most optical sources used in biomedical applications, such as those employed in phototherapy. Providing this average value, in addition to the full spectral data, simplifies the analysis and interpretation of the spectral information, offering a convenient (but not accurate) single metric.

Besides $R_S^{45^\circ}(\lambda)$, we have also characterized the total and specular reflection at smaller angles (30°), labeled as $R_S^{30^\circ}(\lambda)$, in the range of 2.4-25 μm . This extends the characterization of the optical properties of the materials up to 25 μm , thereby encompassing the emissions of lasers extensively used in biomedical applications such as CO_2 (10 μm) and Erbium (2940 nm).

As for reflection, also in the case of transmission, we can identify two contributions: diffusive and ballistic transmission. Ballistic transmission $T_B(\lambda)$ refers to light that passes through a medium without being scattered or absorbed, maintaining its original direction and coherence as it travels through the material. In contrast, diffusive transmission $T_D(\lambda)$ occurs when light propagates through a medium and undergoes multiple scattering events, causing it to spread out and diffuse in different directions. The total transmission is determined by the sum of these contributions:

$$T_{Tot}(\lambda) = T_B(\lambda) + T_D(\lambda) \quad (5)$$

Equipment

Small sample measurements (dimensions of a few centimeters) were performed with a Lambda900 spectrophotometer (Perkin Elmer) equipped with a 150-mm internal diameter integrating sphere (Pela 1000, Perkin Elmer) coated with Spectralon® (LabSphere), a perfectly diffusing material with an optical behavior known as Lambertian, since it homogeneously diffuses light in all directions. By covering each port with the same white material as the sphere, except for the entrance and detector port, a 100% reflectance measurement can be obtained. Inserting a sample into the sample port allows for measurement of total reflectance, which includes both specular and diffuse components. As anticipated, to isolate specular reflectance, a black trap is placed in the specular port, thereby measuring only diffuse reflectance. Specular

reflectance is then calculated by difference. All the reflectance measurements are calibrated against diffusive reflectance standard made of Spectralon® (LabSphere). The Lambda900 spectrophotometer is a dual beam scanning spectrometer with a double grating for stray light reduction, operating in the wavelength range 0.20-2.5 μm , i.e. covering part of the ultraviolet range (UV: 200-380 nm), the whole visible spectrum (VIS: 380-750 nm) and the near-infrared range (NIR: 0.75-2.5 μm).

For measuring the total and specular reflectance on materials that cannot be reduced to small dimensions (e.g. wall plaster) the portable AvaSpec 2048 Standard Fibre Optic Spectrometer manufactured by Avantes (USA) was used.

The AvaSpec 2048 spectrometer performs measurements in the range of 200-1100 nm with a maximum stray light of 0.1%. Its A/D converter is 14-bit @ 1.3 MHz. The sensor is a linear CCD array of 2048 pixels with a signal-to-noise ratio of 200:1. The integration time can be varied from 2 ms to 60 s. For reflectance and transmission measurements, the spectrometer is coupled with different light sources: a fiber-optic illuminator powered by a halogen lamp AvaLight-HAL (Avantes), for the VIS and NIR, and a deuterium-lamp based illuminator AvaLight-DHc (Avantes), for the UV.

To accurately measure total reflectance (*i. e.* total hemispherical reflectance), diffuse reflectance, and transmittance, an integrating sphere was employed. This consists of a spherical cavity with a diffuse white interior surface that, ideally, uniformly scatters incoming light without absorbing it on the whole spectral range of interest. Our integrating sphere is internally coated with Spectralon® (LabSphere). The sphere also includes specific access for light entry (“entrance port”), sample placement (“sample port”), and a light detection port. Optional access can collect the specularly reflected light from the sample (“specular reflection gate”), which can alternatively be excluded from measurement by use of a light black “trap” geometrically positioned in correspondence to the specularly reflected beam.

In the case of the AvaSpec 2048 spectrometer, an integrating mini-hemisphere has been employed. Illumination and detection fibers were coupled with the mini-hemisphere to be 90° apart and to form a 45° angle between the hemisphere plane and each fiber.

Finally, measurements in the range of 2.4-25 μm were conducted using the FTIR spectrometer Nicolet iS50 (Thermo Scientific) using an integrating sphere (Pike). Total $R_{TOT}(\lambda)$ and small-angle $R_S^{30^\circ}(\lambda)$ reflectance measurements were performed with Pike gold-coated sphere and accessory Pike 30Spec.

Results and Discussion

The results are presented as reflectance spectra, including both specular and total reflectance, as well as the Lambertian parameter for all tested materials. Additionally, transmission spectra are provided for various fabric tissues commonly used in clinical operating rooms or in environments where both coherent and non-coherent laser sources are employed. The accuracy of these measurements has been determined to be $\pm 2\%$ for transmission and $\pm 4\%$ for reflection measurements across the entire spectral range examined. This consistency was observed across materials with varying compositions and surface characteristics. The high accuracy, together with reproducibility, indicates the reliable performance of the measurement setup, ensuring that the data accurately reflects the optical properties of the materials under study.

To provide a comprehensive characterization of surfaces pre-

sent in environments where optical radiation is used, we selected a wide range of different samples: metals (with varying degrees of surface finish), transparent and non-transparent plastic materials, building materials, and fabrics specific to biomedical applications or operating rooms (Table 1).

In Figure 2 we report the total and specular reflectance, together with the Lambertian spectral parameters and the total reflectance in the NIR for several metals, with both polished and brushed surface finishing, and some plastic materials.

Reflection spectra show great variability: surface characteristics (material composition and surface treatment) play an important role in the determination of the spectral reflectance curves. The wavelength dependence must also be carefully considered because the same sample can behave very differently at different wavelengths. This indicated that the material reflection properties in the UV or IR range cannot always be deduced from the visible range, as can be seen in several materials shown in Figure 2.

Polished materials, as expected, exhibit significantly higher specular reflectance compared to satin-finished ones. Notable differences are observed between near IR and mid-IR (up to $\lambda=25 \mu\text{m}$). In particular, brushed metals demonstrate a small-angle reflection that is several tens of percentage points higher in the 10-25 μm range. This range is of particular interest for clinical and industrial settings because it includes CO₂ laser emission. Brushed metals also show up to 10% specular reflection in the visible wavelengths, a value that in many cases cannot be neglected in risk management. Regarding the plastics, we observe that their behavior is predominantly diffusive within the measured range. In determining the $L_{LAMB}(\lambda)$ parameter, we note that this parameter reaches

values greater than 100, its theoretical maximum, around the region of 2 μm . This is due to the limited accuracy of the reflectance measurement, which, for some materials, leads to a slight overestimation of specular reflectance compared to the total reflectance (always within the stated accuracy $\pm 4\%$). This can result in $L_{LAMB}(\lambda)$ values exceeding 100. In Figure 2 we can identify the diffusive/specular behavior (at 45°) of different materials by looking at the $L_{LAMB}(\lambda)$ value: the smaller it is, the more diffusive the material is.

In Figure 3, we present the total reflectance spectra $R_{Tot}(\lambda)$ in the two ranges of 250-2500 nm and from 1.5 μm up to 25 μm , again examining various fabrics with significantly different textures and composition (see Table 2 for additional information) to obtain a representative sample of those used in environments where optical radiation sources are present, with particular reference to the hospital setting. We also measured the specular reflection in the 250-2500 nm range. All measured textile samples exhibited very similar behavior in terms of total reflection. As shown in Figure 3, the total reflectance in the range of 250-2500 nm shows an initial peak in the visible spectrum reflecting the coloration of the material (generally blue or green). Then, a higher plateau starts from around 700 nm, varying from approximately 60% to almost 90% (depending on the type of fabric), gradually decreasing at longer wavelengths. Furthermore, the specular reflectance of all fabrics was found to be less than 4% (limited by instrumental accuracy alone) in the range of 250-2500 nm. However, considering the surface finish of the fabrics and, consequently, the representative length of surface irregularities, very low values of specular reflectance are also expected in the range up to 25 μm . Therefore,

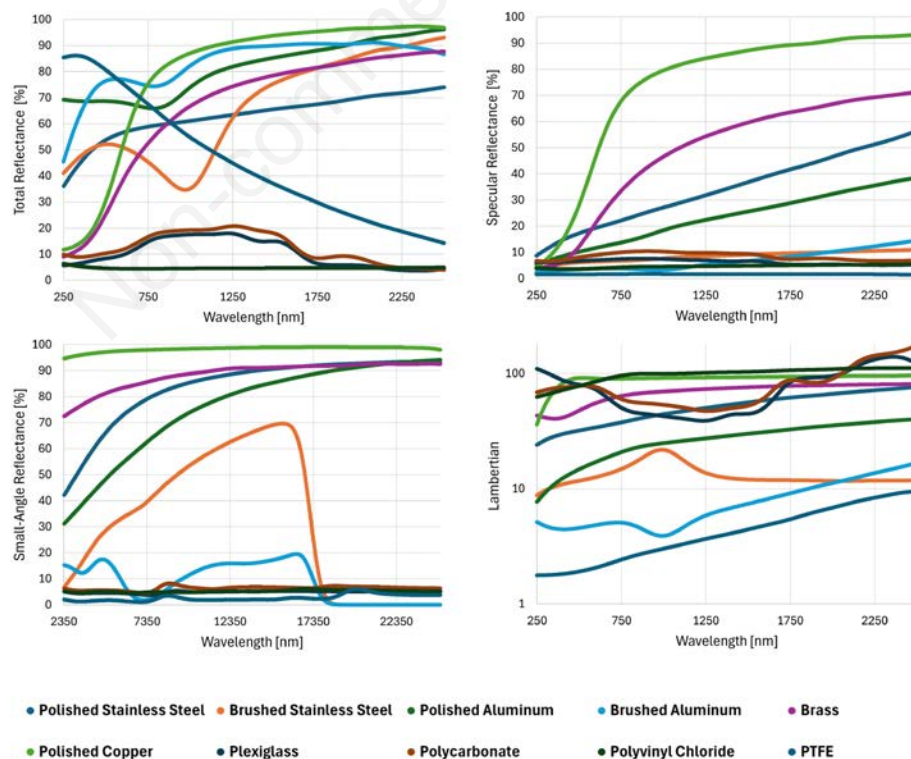


Figure 2. Specular $R_S^{(45^\circ)}(\lambda)$ and total reflectance spectra $R_{Tot}(\lambda)$, together with the Lambertian parameter $L_{Lamb}(\lambda)$ in the spectral range 250-2500 nm. Small-angle reflectance spectra $R_S^{(30^\circ)}(\lambda)$ is reported in the wavelength range 1280-25000 nm.

the behavior of the fabrics is highly diffusive, with total reflectance values potentially exceeding 80%. Although diffusely reflected radiation is less hazardous than specular radiation, contrary to expectations textile surfaces can have a diffusive reflectance comparable to satin-finished metals, which must be properly accounted for in risk assessment.

As an example, in Figure 3, we also compare the total reflectance $R_{Tot}(\lambda)$, the total $T_{Tot}(\lambda)$ and ballistic $T_B(\lambda)$ transmittance, and the absorbed fraction $A(\lambda)$ for textile samples A and C. The specular reflectance is not reported, being below the instrument's accuracy limit as previously mentioned. The ballistic transmittance, like the reflectance, is heavily attenuated, resulting in a predominant contribution from diffuse transmittance. All the tested fabrics exhibit spectra analogous to those reported.

Table 2 reports on the $I_{Lamb}^{400-1100\text{ nm}}$ value, calculated as the average of the spectral curve $L_{LAMB}(I)$ over the range 400-1100 nm, together with the surface roughness parameter R_a for metallic sam-

ples.¹¹

The values for the metals indicate that aluminum exhibits greater diffusivity compared to steel, both in its polished and satin-finished forms. It is important to note that the parameter does not represent the absolute diffusive or specular properties of the sample. The significant variability in the values of $R^{45^\circ}(\lambda)$ and $R_{Tot}(\lambda)$ across different wavelengths, both in the visible and infrared regions for certain materials, necessitates a meticulous evaluation of this Lambertian value at the specific wavelengths or emission bands of the sources. This is crucial for accurately assessing the potential ocular hazard.

Finally, for completeness, we present the optical properties of a highly transparent material such as glass. Specifically, we have examined BK7 crown glass, a standard material for optical equipment. BK7 is commonly used in the production of lenses, foils, and prisms for ophthalmology, as well as in the lenses of cameras and microscopes. This glass exhibits greater transparency in both the

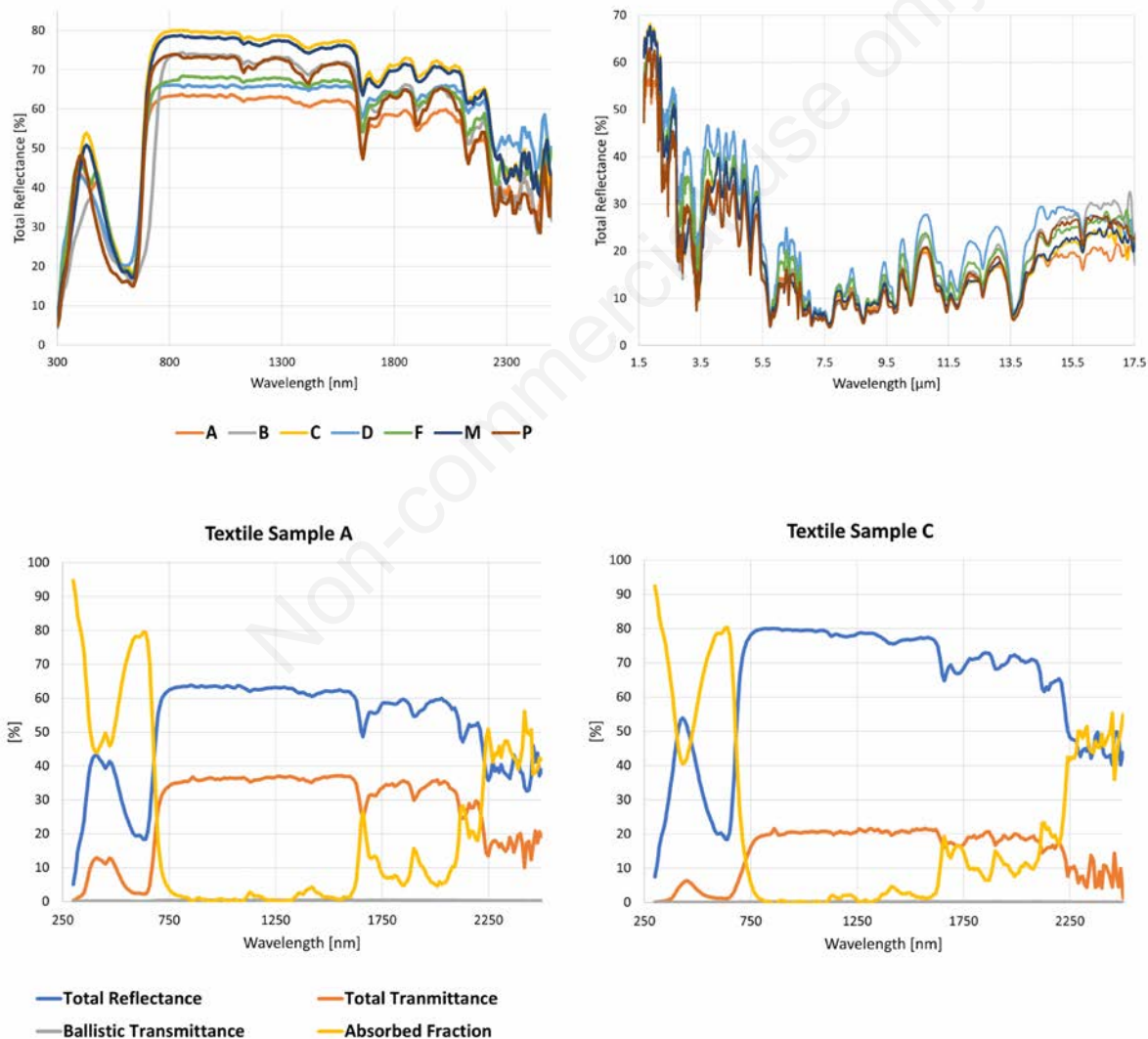


Figure 3. Total reflectance spectra $R_{Tot}(\lambda)$ in the spectral range 250-2500 nm and total reflectance spectra in the wavelength range 16-20 μm . All the tested blue-coloured textiles show specular reflectance lower than the instrument accuracy in the 250-2500 nm range ($R_S(\lambda) < 4\%$) and has not been reported in the graph. In the same spectral range we report an example of total $T_{Tot}(\lambda)$ and ballistic transmission $T_B(\lambda)$ together with the absorption curve $A(\lambda)$ and the total reflectance $R_{Tot}(\lambda)$ for textile samples A and C.

Table 1. Macroscopic (3x3 cm²) and microscope images of the different blue-coloured textiles tested in this work. Green-coloured textiles were also tested, showing the same composition and surface finishing of the ones reported above (data not shown).

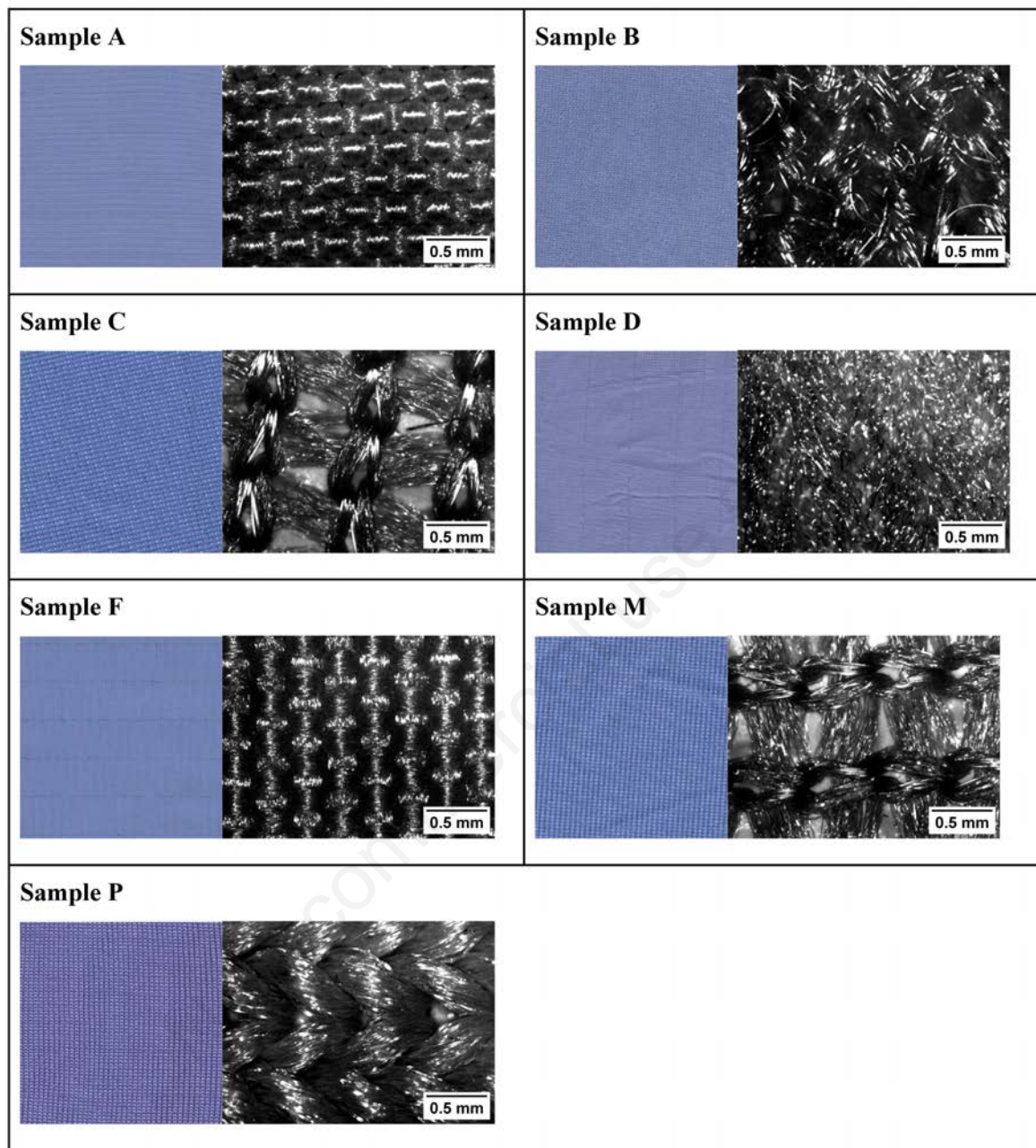


Table 2. Average values of L_{Lamb} (λ) in the range 400-1100 nm (indicated as $L_{Lamb}^{400-1100\text{ nm}}$) and the surface roughness parameter R_a for metallic samples. For textiles, the value has been estimated assuming a 4% specular reflectance that corresponds to the measuring instrument limit.

Sample	$L_{Lamb}^{400-1100\text{ nm}}$	R_a [μm]	Sample	$L_{Lamb}^{400-1100\text{ nm}}$	R_a [μm]
Polished Stainless Steel	38	0.12	Brushed Stainless Steel	16	0.68
Polished Aluminum	20	0.35	Brushed Aluminum	5	0.41
Brass	60	0.14	Polished Copper	90	0.06
Plexiglass	58	–	Polycarbonate	64	–
Polyvinyl Chloride	91	–	PTFE	2	–
Textiles A	< 10	–	Textile C	< 8	–

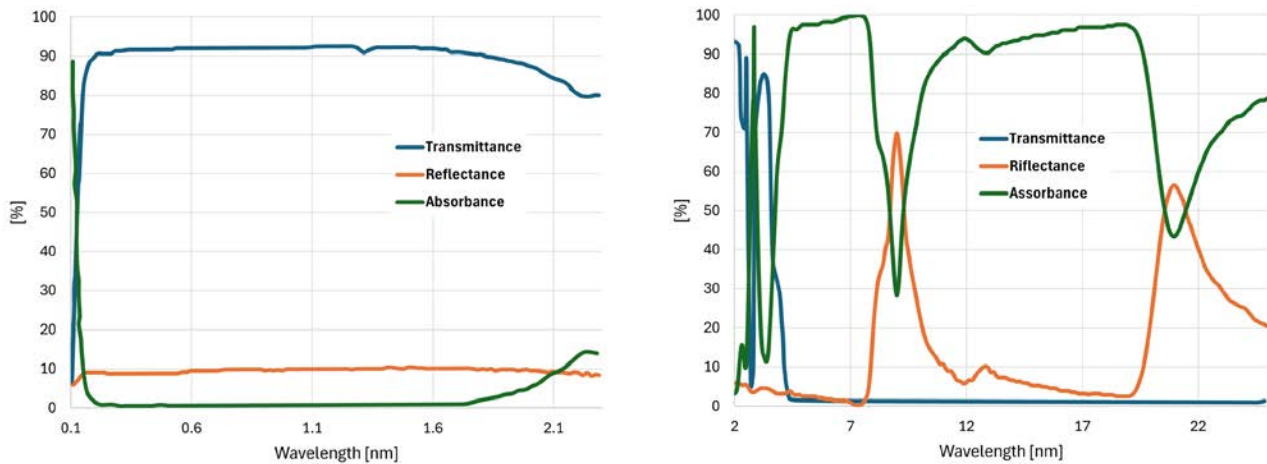


Figure 4. Optical properties diagram of a 10-mm thick BK7 borosilicate glass sample from Schott.

visible and infrared spectra compared to ordinary ‘green’ window glass. As shown in Figure 4, the reflectivity of BK7 is expected to be less than 10% over the entire visible range. However, there are two bands of high reflectivity in the infrared spectrum, between 7.5 μm and 11 μm , and between 19 μm and 25 μm .

The presence of these two bands in the infrared region underscores the importance of accurate characterization of the optical properties of materials: extrapolating, for instance, the reflectance behavior of one spectral region to another can lead to significant errors and underestimations. This inaccuracy is particularly critical when the data are used to determine safety criteria for laser radiation and to implement measures ensuring the safety of workers in environments where optical radiation is utilized.

Conclusions

The reflective properties of materials used in the biomedical environment are of great interest for risk management purposes when laser light and other non-coherent sources are used in clinical practice or research. When light from a laser source hits a surface, it produces both specular and diffuse reflections, which can have harmful effects, particularly on the eyes. While diffusely reflected radiation is generally less hazardous than specular radiation, it is important to note that textile surfaces can exhibit a diffusive reflectance comparable to that of satin-finished metals. This unexpected characteristic must be carefully considered in risk assessments. Of particular interest is the comparison of different L_{LAMB} (λ) curves and values, which were presented in correspondence to the laser wavelengths most commonly used in clinical practice and provide an immediate index that indicates whether a given surface behavior is mainly diffuse or specular. Based on the results presented here, the creation of a database of material reflective properties has been initiated.¹²

References

1. Barat K. Laser Safety: Tools and Training. 2nd ed. London (UK): Taylor & Francis Ltd, 2017.
2. Directive 2006/25/EC of the European Parliament and of the Council of 5 April 2006 on the minimum health and safety requirements regarding the exposure of workers to risks arising from physical agents (artificial optical radiation) (19th individual Directive within the meaning of Article 16(1) of Directive 89/391/EEC). Non-binding guide to good practice for implementing Directive 2006/25/EC 'Artificial optical radiation'. Publication Office of EU (2011) ISBN 978-92-79-16046-2 doi:10.2767/742018.
3. International Commission on Non-Ionizing Radiation Protection (ICNIRP). ICNIRP Guidelines on Limits of Exposure to Laser Radiation of Wavelengths between 180 nm and 1,000 μm . Health Phys. 2013 Sep;105(3):271-295.
4. European Normative: EN 60601-2-22. Medical electrical equipment - Part 2-22: Particular requirements for basic safety and essential performance of surgical, cosmetic, therapeutic and diagnostic laser equipment.
5. Niemz MH. Laser-tissue interactions: fundamentals and applications. Springer. 2019.
6. Inero G, Fusi F, Romano G. The safe use of lasers in biomedicine: Principles of laser-matter interaction. J Public Health Res 2023;12:22799036231187077
7. Cimmino MC, Biondi M, Guasti A, et al. Laser interaction with medical textiles: changes of optical properties and damage thresholds. Physica Medica: Eur J Med Physics 2023;115:102884.
8. Romano G, Inero G, Marrugat SN, Fusi F. Innovative light sources for phototherapy. Biomol Concepts 2022;13:256-71.
9. Vo-Dinh T (ed). Biomedical Photonics Handbook. Boca Raton: CRC Press, 2003.
10. Vo-Dinh T (ed). Biomedical Photonics Handbook: Therapeutics and Advanced Biophotonics. 2nd ed. Boca Raton: CRC Press, 2014.
11. ISO 21920-2:2021, Geometrical product specifications (GPS) — Surface texture: Profile
12. Material reflectance database. Available from: https://www.portaleagentifisici.it/fo_ro_artificiali_riflettanza_materiali.php?lg=EN